ULTRASONIC TREATMENT OF PET/LCP BLENDS DURING EXTRUSION

*Kaan Gunes and A. I. Isayev**
Institute of Polymer Engineering
The University of Akron
Akron, Ohio 44325-0301

* Corresponding author: aisayev@uakron.edu

Abstract

Wholly aromatic liquid crystalline copolyester was blended with PET to produce self-reinforced composites using ultrasonically assisted single screw extrusion. Ultrasonic amplitude and residence time in the sonication zone were varied to induce in-situ compatibilization in the blends. Increasing ultrasonic power was found to decrease pressure upstream of the ultrasonic treatment zone. Rheological, mechanical and morphological properties of the ultrasonically treated blends were studied. Ultrasonic treatment at an amplitude of 7.5 μm caused an increase in viscosity of PET and PET/LCP blends. Cole-Cole plots indicated increased elasticity of PET and molecular changes in the blends with ultrasonic treatment. An improvement in mechanical properties of LCP and some PET/LCP blends was observed. Ultrasonic treatment of 90/10 PET/LCP blends at high amplitudes led to the creation of hairy surfaces on LCP droplets in the core region of moldings. LCP fibrillation in the skin region of PET/LCP moldings is not observed at high ultrasonic amplitude and long residence time. Ultrasonically treated blends indicated improved interfacial adhesion over those without treatment. The observed changes in PET, LCP and their blends suggested that ultrasonic treatment in the melt state induced homopolymerization of PET and copolymerization of PET/LCP blends, through possible esterification and transesterification reactions.

Keywords: thermotropic LCP; PET; ultrasound; blends; interfacial adhesion

Introduction

Liquid crystalline polymers (LCP) have excellent mechanical properties in addition to their superior dimensional, thermal and chemical stability. Blends of these materials with other LCPs or thermoplastics form self-reinforced or in-situ fiber-reinforced composites during processing and are sought to replace traditional fiber-filled composites due to their ease of processing. LCPs are ideal for applications in aerospace, automobile, marine, sports and other markets requiring high performance materials [1-4].

The widespread use of LCPs is hindered by their high cost, promoting the study of their blends with conventional thermoplastic polymers. Unfortunately, commercial LCPs are immiscible with many thermoplastic polymers. The challenge in the processing of thermoplastic/LCP blends is to increase the interfacial adhesion between the blend components while preserving the in-situ formation of rigid LCP fibrils. The latter is affected by volume fraction, viscosity ratio of the components and processing conditions. An optimum amount of compatibilization is necessary to fully utilize these blends [2, 5-10].

Previous researchers have studied compatibilization of blends of commercial LCPs with thermoplastics [2, 7, 9-15]. Among the methods used are prolonged annealing [7], use of catalysts [10], introduction of block-co-polymers into the blends [11, 12], substitution of flexible groups on LCP main chain [13, 14] and addition of acids [15] to promote transesterification in blends. In the case of polyester/LCP blends, transesterification reactions in the melt state through annealing and high temperature processing in batch mixers for prolonged periods create copolymers with molecular affinity to both phases of the blends [2, 7]. On the other hand, excessive transesterification of polyester/LCP blends are shown to hinder phase separation and LCP fibrillation and reduce mechanical properties of compatibilized blends [9]. While addition of catalysts can increase the speed of copolymerization in these blends, these reactions are carried out in batches and controlling the extent of copolymerization to yield superior blends is difficult.

High power ultrasound acting on the melt is known to cause chain scission and initiate reactions in polymers [16-22]. Application of ultrasonic energy leads to cavitation through the generation of alternating compression and rarefaction waves, which in turn form bubbles that pulsate and grow. When cavitating bubbles collapse, they generate local hotspots of extreme temperature and pressure, where reactions can take place. Acoustic cavitation is concentrated in material defect sites, such as inhomogeneities and multiphase interfaces [20, 21]. Depending on the amplitude of ultrasonic waves and the chemical structure of the polymer, recombination of chains can take place and high molecular weight polymer chains can be generated [16-19, 22]. High power ultrasound was found to promote reactions leading to copolymerization in immiscible rubber/rubber [16, 18], rubber/plastic [16] and plastic/plastic [17] blends. Homopolymerization reactions are also promoted by applying ultrasound and are not necessarily limited to free radical polymerization, as documented by the significant molecular weight increase of PA6 following sonication in the extrusion of PA6/PP blends [17]. These reactions occur during melt processing in the ultrasonic treatment zone of an extruder at very short residence times.

The study of ultrasonic treatment on polyester/LCP blends is of particular interest as the continuous compatibilization of these blends would allow the production of high performance materials with superior mechanical properties and increase their areas of application [19]. In this article, we study the effects of high power ultrasound on the morphology, rheology, and mechanical properties of PET, LCP and their blends.

Experimental

Materials

The liquid crystalline polymer (Vectra A950, Ticona) used is a wholly aromatic copolyester containing 73% hydroxyl benzoic acid and 27% hydroxyl naphthalic acid [23]. The polyester PET

(Eastapak PET 7352, Eastman Chemical Company) was chosen as the matrix in the blends. Its intrinsic viscosity is 0.74 dl/g. Both resins were acquired in pellet form and were dried at 120^{o}C in a vacuum oven (Fisher Scientific, Isotemp 285A) at a gauge pressure of -710 mmHg for 24 hours prior to use. A similar drying procedure was repeated on prepared blends prior to further processing and characterization.

Preparation of PET/LCP Blends

For the blending of PET and LCP, a new ultrasonic single screw extruder was designed. Its schematic is presented in Fig. 1. A commercially available extruder (KL100, Killion) having a diameter of 25.4 mm (1 in) was modified by adding ultrasonic treatment sections. The extruder was fitted with a new screw having an L/D ratio of 33:1. The screw had three mixing sections. The first was a 5.38 cm long Union Carbide Mixer (UCM) located 41.8 cm from the start of the screw. The second was a 6.35 cm long Melt Star Mixer (MSM) located 7 cm after the first. These two mixing sections were placed before the ultrasonic treatment zone. Finally, the third was a 6.35 cm long MSM at the discharge end of the screw after the ultrasonic treatment zone. The barrel temperature was set at 260°C in the feeding zone and 285°C in all other zones. These processing temperatures were chosen to minimize degradation of the PET component while ensuring the LCP is processed in the nematic phase. The ultrasonic zone, located at a distance of 73 cm from the feed end of the screw, was preceded by a flightless section of the screw where a pressure transducer (Dynisco PT435A) was mounted onto the barrel. Pressure, barrel temperature and ultrasonic power consumption were recorded by computer through a data acquisition system (Dataq Instruments, DI-715-U) at an acquisition rate of 2 data points per second.

The ultrasonic system was composed of two identical sets of 20 kHz power supplies (Branson 2000bdc), fan cooled ultrasonic converters (Branson H.P. 101-135-124), 1:1 titanium boosters (Branson 101-149-096) and aluminum ultrasonic horns of 2.54x2.54 cm^2 cross section. The horns have tips with a radius of curvature of 1.8 cm matching that of the barrel curvature in the treatment zone. For all

ultrasonic treatment experiments, both horns were operated simultaneously. The ultrasonic power imposed on the melt was controlled by adjusting the amplitude dials on the ultrasonic power supplies. The amplitude at the tip of the horns was calibrated in air in the range of 0-15 μm. The horns were mounted symmetrically onto the barrel. Both horns were cooled with tap water at a flow rate of 1 cm^3/min in order to prevent the ultrasonic system from overheating. Streamlined reliefs on the sides of the barrel in the ultrasonic treatment area guided the polymer melt to flow equally through the two channels of 2.54 mm (0.1 in) thickness between the ultrasonic horns and the screw. Polybenzimidazole (Celazole, PBI Performance Products Inc.) seals of 4 mm thickness were mounted in the barrel around the ultrasonic horns to prevent leakage of polymer melt.

The flow rate was varied to study the effect of residence time of the melt in the ultrasonic treatment zone. Under flood feeding conditions, screw speeds of 15 and 7 RPM gave mass flow rates of 1 and 0.5 kg/hr, resulting in mean residence times of 7 and 14 s, respectively. It should be noted that the experiments at a flow rate of 0.5 kg/hr were conducted only on the 80/20 PET/LCP blend. A circular die of 2 mm diameter with a L/D ratio of about 6.4, preceded by a converging circular section, was attached to the end of the extruder. Melt exiting the die entered a water bath kept at room temperature. Solidified polymer was then collected, dried, and subsequently pelletized in a grinder (Weima, WSL180/180).

Impact bars (63.50 x 12.70 x 3.18 mm^3, ASTM D 256-05) and dumbbell shaped mini tensile bars (63.50 x 9.53 x 1.52 mm^3, ASTM D 638-03) were injection molded simultaneously using a Van Dorn 55 HP-2.8F injection molding machine. The barrel temperature was set at 285°C in all zones except the feeding zone, which was set at 260°C. The mold was kept at room temperature. Other injection molding parameters were: a clamping force of 55 tons, an injection speed of 15 cm/s, holding pressure of 4 MPa that was applied for 20 s, and a cooling time of 40 s.

A compression molding press (Carver 4122) was used to prepare discs for rheological testing. Four discs 2 mm in thickness and 25 mm in diameter were molded at 280°C for PET and blends and at 300°C

for pure LCP. The mold and metal plates were sprayed with high temperature mold release agent (Frekote HMT2), and Kapton® polyimide film (Dupont) was placed between the preheated platens and the mold. Following preheating of pellets in the mold for 2 min, a force of 1 ton was applied for 50 s and released for 10 s for 3 consecutive times. After that, a force of 5 tons was applied for 2.5 min and released for 10 s, this time for two consecutive times. The hot metal plates and the mold were removed from the press and allowed to cool for 8 minutes. The discs were then removed from the mold.

Rheological Measurement

An Advanced Rheometric Expansion System (ARES, TA Instruments) rotational rheometer was used in oscillatory shear mode with parallel plate geometry. Dynamic frequency sweep experiments with angular frequency (ω) of 0.1 to 100 s^{-1} were performed at a strain amplitude of 2% and a temperature of 280^{o}C. Pure PET and all blends were tested in a nitrogen atmosphere, while pure LCP, which was found to be stable in air at high temperatures for the duration of measurements, was tested in an air environment. The complex viscosity ($|\eta^*|$), dynamic storage (G') and loss (G'') moduli were obtained. All reported rheological values are averages of four tests. A percentage error (standard deviation/average) was 5% for PET and blends, and 10% for LCP.

Spectroscopic Studies

Attenuated total reflectance Fourier transform infrared spectroscopy (Thermo Nicolet FT-IR with smart orbit ATR module) was carried out using 32 scans at a resolution of 4 cm^{-1} on compression molded PET and blend specimens. In case of the blend, PET phase was extracted using a Soxhlet extraction apparatus by refluxing boiling m-cresol for 48 hours through a cellulose thimble. Undissolved fraction of blend was collected and compression molded for FT-IR study.

Morphological Studies

Morphological studies of the blends were performed using a Hitachi S-2150 scanning electron microscope (SEM). Mini dumbbell shaped samples were fractured at the center after soaking in liquid

nitrogen for 5 minutes. The fractured sample was then mounted onto a metal holder and the fracture surface was coated with platinum using a sputter coater (Emotech, K575X). Since molded blend specimens exhibited skin-core morphology, micrographs were captured in both of these regions.

Mechanical Tests

An Instron 5567 tensile tester was used to study the tensile properties of injection molded mini tensile bars following ASTM D 638-03 at a crosshead speed of 5 mm/min. The test specimens were mounted using mechanically tightened side action grips. A 30 kN load cell was used. The Young's modulus was obtained using an extensometer having a gauge length of 7.62 mm. As the extensometer was acted as a stress concentrator, tensile tests to obtain values of the strength and elongation at break were carried out without it. A minimum of 6 samples were measured and subsequently averaged. Percent error (standard deviation/average) of less than 3, 7, 10 and 20% were obtained for the ultimate strength, Young's modulus, elongation at break and toughness, respectively.

Impact testing of the injection molded samples was carried out using an Izod impact tester (Testing Machines Inc., 43-1) with a 907 g load for the blends, and a 4536 g load for pure LCP. Since specimens of the blends were too brittle with notching, the unnotched specimens were used in order to improve accuracy of the measurements. ASTM D-256-05 procedure was followed except for notching. Pure PET did not break without notching. Therefore, its impact strength could not be compared with that of the blends and its value was not reported. The values reported are the averages of at least 20 tests. Percent error (standard deviation/average) of 10 and 25% were obtained for blends and LCP, respectively.

Results and Discussion

Process Characteristics

Fig. 2 shows the ultrasonic power consumption as a function of LCP concentration at different ultrasonic amplitudes for a flow rate of 1 kg/hr. This figure also shows variation of the ultrasonic power

consumption with amplitude for 80/20 PET/LCP blend at a flow rate of 0.5 kg/hr. Ultrasonic power consumption increased with ultrasonic amplitude, due to increased strain amplitude imposed on the melt, and with flow rate, due to increased pressure acting on the melt. With the addition of LCP it goes through a maximum at certain LCP concentration depending on ultrasonic amplitude. This maximum is most prominent for 80/20 and 70/30 PET/LCP blends, processed at a flow rate of 1 kg/hr and an ultrasonic amplitudes of 7.5 μm and 10 μm signifying a greater effect of ultrasound under these conditions. The higher ultrasonic power consumption observed in some blends could be due to the increased number of defect sites available for acoustic cavitation at the interface of immiscible polymers. The morphology of the blend and the nature of the pure components do affect acoustic cavitation and resulting power consumption.

Fig. 3 shows the pressure before the ultrasonic treatment zone of the extruder as a function of LCP concentration for different ultrasonic amplitudes at a flow rate of 1 kg/hr. This figure also shows the pressure values obtained for 80/20 PET/LCP blend at a flow rate of 0.5 kg/hr. As expected, pressure is lower at lower flow rate. For each blend composition, the pressure is found to decrease with increasing ultrasonic amplitude. Therefore, there is a possibility for increased output in extrusion with the application of ultrasonic energy. As acoustic cavitation in the melt results in both permanent and thixotropic changes in viscosity [22], the net effect on pressure is determined by these two competing effects. In ultrasonic extrusion, there is also a possible slip of polymer melt along the surface of the horns, which can further lead to a decrease in pressure [18]. Concerning the effect of LCP concentration on pressure, the presence of a maximum and a minimum pressure is noted depending on concentration and ultrasonic amplitude. At an amplitude of 10 μm the pressure continuously increases with concentration. At other amplitudes there is a non-monotonous variation of the pressure with LCP concentration due to variation of the effect of ultrasound at different blend compositions. Such a variation of pressure can be attributed to the sensitivity of pressure to the melt temperature during

extrusion. It should be noted that variation in the barrel temperature during experiments was less 2^{o}C. However, temperature variation in the melt located under the ultrasonic horns may occur. Unfortunately, the melt temperature in this region could not be measured. The melt temperature variation may take place due to flow of cooling water through horns. At different ultrasonic amplitudes it may lead to a change of cooling conditions on the horn. Also, with increasing amplitude, horns may become hot and therefore affect the melt temperature. In addition, to avoid excessive degradation of PET, the processing temperature (285^{o}C) was chosen relatively close to the solid to nematic phase transition temperature of the LCP (280^{o}C) [24]. In this temperature region, the sensitivity of viscosity to temperature is most pronounced and therefore may contribute to the complexity of the observed pressure variation.

Rheology

Rheological property measurements were performed under dynamic conditions, in contrast to steady-state conditions that require a longer testing time. This was done in order to avoid PET degradation and to reduce changes in LCP texture. Figures 4a and 4b show the complex viscosity of the blends treated at different ultrasonic amplitudes at a flow rate of 1 kg/hr varies with increasing LCP concentration at frequencies of 1 s^{-1} and 100 s^{-1}, respectively. In contrast to the maximum relative error of 5% in viscosity for samples of pure PET and the PET/LCP blends, an error of 10% was recorded for samples of pure LCP. Similar variations in LCP viscosity measured by rotational rheometry have been documented by other researchers [25, 26]. This was attributed to the proximity of the testing temperature to the nematic transition temperature of the LCP [25], differences in sample texture due to the presence of oriented domains [25, 26], the inability to remove residual normal stresses at the start of testing and off-gassing of the compression molded discs during testing [27]. Considering the experimental deviation in LCP viscosity measurements, it can be stated that no noticeable changes in the viscosity of LCP under ultrasonic treatment were observed.

While the pressure during extrusion was observed to decrease with ultrasonic amplitude, it can be seen from Fig. 4b that the viscosity of pure PET as well as 90/10, 80/20 and 60/40 PET/LCP blends at a flow rate of 1 kg/hr were higher at a frequency of 100 s^{-1} after treatment at an amplitude of 7.5 μm. Similar observations can be made in Fig. 4a for pure PET and 90/10 PET/LCP blend at a shear rate 1 s^{-1}. The observed increase of viscosity of the PET and PET/LCP blends after their ultrasonic treatment seems to be in contradiction with pressure reduction with the increase of ultrasonic amplitude (Fig. 3). The latter clearly indicates that thixotropic and slip phenomena are the dominating factors in pressure reduction with ultrasonic amplitude during extrusion. The pressure data of Fig. 3 and the rheological data of Figs. 4a and 4b show that ultrasound has a complex effect on the pressure and viscosity variation of PET/LCP blends. The effect of ultrasound on polymer blends depends on the ultrasonic amplitude, nature of components, blend composition and extent of ultrasonically induced chemical changes.

It is known that high intensity ultrasound leads to chain scission in long chains polymers [16-22]. It is also documented that this can lead to the formation of lower molecular weight species, as well as high molecular weight fractions and copolymers through the generation of active sites by chain scission and subsequent recombination reactions [16-22]. The above mentioned increase of viscosity of PET and PET/LCP blends at an ultrasonic amplitude of 7.5 μm points toward the recombination of chains, which leads to molecular weight buildup, probably through esterification of PET and copolymerization at the interface of PET/LCP blends in the melt state [19-22]. On the other hand, pure PET and all of the blends are found to exhibit the lowest viscosity following ultrasonic treatment at an amplitude of 10 μm, indicating a reduction in molecular weight by permanent chain scission at this high amplitude. These findings suggest that ultrasonic amplitude controls the competition between chain scission and molecular weight buildup in this system.

Comparing the viscosity of PET at frequencies of 1 s^{-1} (Fig. 4a) and 100 s^{-1} (Fig 4b), it is seen that they are nearly the same since PET exhibits Newtonian behavior. On the other hand, the LCP phase

exhibits strong shear thinning behavior [2, 28, 29]. This explains why the viscosity of the blends at ω = 100 s^{-1} is lower at higher concentrations of LCP in the blends. It is also seen that the viscosity of the 90/10 and 80/20 PET/LCP blends is less than that of the pure components. This is due to the action of LCP as a flow modifier [2, 30, 31]. Evidently, orientation of the LCP phase in the flow direction reduces melt viscosity, as observed in both capillary and rotational rheometry experiments [29].

With reference to Fig. 4b, it can be seen that the viscosity of untreated 80/20 PET/LCP blends is higher at the lower flow rate of 0.5 kg/hr. This indicates that the polymer degradation during extrusion is less at lower flow rate. This mechanically induced degradation could be due to the presence of shear intensive mixing sections on the screw. It is also worth noting that the viscosity of 80/20 PET/LCP blend processed at a flow rate of 0.5 kg/hr and treated at an ultrasonic amplitude of 10 μm is slightly higher than that of the same blend treated at 7.5 μm. This behavior in viscosity is different than that observed at a flow rate of 1 kg/hr. The observed increase in viscosity at a flow rate of 0.5 kg/hr and at an ultrasonic amplitude of 10 μm indicates formation of high molecular weight components through chemical reactions in the melt. Moreover, the difference in viscosity with processing at different flow rates signifies that ultrasound of given amplitude affects the same material differently depending on the residence time in the ultrasonic zone. Ultrasonic treatment results in degradation of polymer chains leading to generation of reactive species. For the blends under study, these species can initiate polycondensation reactions through recombination of hydroxyl and carboxyl terminal groups leading to an increase in molecular weight of homopolymers and formation of copolymers. This is supported by the observed increases of viscosity of PET and PET/LCP blends after ultrasonic treatment at an amplitude of 7.5 μm. It should be noted that similar reactions were observed in PA6 and PA6/PP blends during their ultrasonic treatment leading to an increase of mechanical properties and viscosity [17].

An attempt was made to determine copolymer formation using the FT-IR studies by comparing FT-IR spectra of untreated and ultrasonically treated blends with and without extraction of PET phase.

However, these studies indicated no noticeable changes in the absorption spectra of the blends after ultrasonic treatment. In particular, no shift of peaks and no new peaks were detected in the FT-IR spectra. It is possible that the ester groups of the LCP and its copolymer with PET overlapped and/or the amount of the copolymer was too small to be detected.

Cole-Cole plots [32] provide important rheological information and can be used to determine structural changes in materials [33-37]. Fig. 5 is a plot of G' vs. G" for PET, LCP and their blends without ultrasonic treatment and with ultrasonic treatment at an amplitude of 7.5 μm. It is seen that the elasticity of the blends increases with LCP concentration. Ultrasonic treatment of pure PET causes G' to increase more than G", such that G' vs. G" plot of the treated PET lies above that of the untreated, showing the increased elasticity of the treated PET. This correlates well with the observed increase in viscosity of PET after ultrasonic treatment, suggesting that ultrasonically induced homopolymerization reactions take place in the melt. In PET/LCP blends, both G' and G" at a fixed circular frequency were observed to increase with ultrasonic treatment indicating the occurrence of structural changes in blends. However, the increase in G' was less than that in G", such that the curves of G' vs G", as shown in Fig. 5, lie lower for ultrasonically treated blends indicating the decreased elasticity of treated blends. In contrast to observed changes in PET and PET/LCP blends, the ultrasonic treatment of pure LCP did not result in any noticeable changes to values of the storage and loss moduli. This indicates that structural changes in LCP under ultrasonic treatment can not be detected through rheological measurements.

Mechanical Properties

Figs. 6a and 6b, respectively, show the tensile strength and Young's modulus as a function of LCP concentration in PET/LCP blends without and with treatment at different ultrasonic amplitudes and at flow rates of 1 kg/hr and 0.5 kg/hr for 80/20 PET/LCP blend. In general, the blends become stronger and more rigid with the addition of LCP. Slight improvements in the tensile strength of 80/20 PET/LCP blends and Young's modulus of both 80/20 and 70/30 PET/LCP blends were recorded at an amplitude of

7.5 μm and a flow rate of 1 kg/hr. However, ultrasonic treatment at an amplitude of 10 μm leads to a significant decrease in the tensile strength and Young's modulus at all concentrations of PET/LCP blends. This indicates that ultrasonic degradation of polymer melt prevails at high ultrasonic intensity. Depending on concentration, ultrasonic treatment at an amplitude of 5 μm is found to slightly decrease or have no effect on the mechanical properties of the blends. It follows that there is a critical ultrasonic amplitude below which changes in molecular structure are not substantial as to have a prominent effect on mechanical properties.

Figs. 7a and 7b show the toughness and impact strength, respectively, as functions of LCP concentration in PET/LCP blends without and with treatment at different ultrasonic amplitudes and at flow rates of 1 kg/hr and 0.5 kg/hr for 80/20 PET/LCP blend. The blends generally become more brittle with the addition of LCP, owing to weak interfacial adhesion between PET and LCP. However, improvements in the toughness of 90/10 PET/LCP blend with ultrasonic treatment at an amplitude of 10 μm, and in the impact strength of 80/20 PET/LCP blend at an amplitude of 7.5 μm show that ultrasonic treatment can reduce brittleness of these immiscible blends, suggesting that the effect of copolymerization in the melt is greater than the degradation of PET under these conditions. On the other hand, ultrasonic treatment at an amplitude of 10 μm led to significant reductions in the toughness of blends containing above 20 wt% LCP, and in the impact strength of all blends. The latter was due to degradation of the PET matrix as indicated by the previously discussed decrease in viscosity with treatment at this amplitude. Apparently, chain scission is the prevailing effect during ultrasonic treatment of these blends at this high amplitude. However, the recorded improvements in some mechanical properties of blends with ultrasonic treatment at certain amplitudes indicate that there is a competition between chain scission and recombination. The observed improvements in the tensile properties of the ultrasonically treated blends are partially due to homopolymerization of the pure PET, as indicated by an increase of its viscosity after ultrasonic treatment at an amplitude of 7.5 μm, shown in

Fig. 4. Improvements in mechanical properties with ultrasonic treatment at certain amplitudes could also possibly be related to transesterification reactions, leading to improved adhesion between PET and LCP as seen from SEM micrographs presented in the next section.

Figures 6 and 7 also demonstrate that 80/20 PET/LCP processed at a feed rate of 0.5 kg/hr have greater toughness and impact strength following ultrasonic treatment at an amplitude of 10 μm, as opposed to 7.5 μm. This result is consistent with the increased viscosity recorded for this blend treated at an ultrasonic amplitude of 10 μm in contrast to 7.5 μm (Fig. 4), indicating that high molecular weight species is evidently formed and compatibilization of the blend is achieved through possible esterification/transesterification reactions in the melt due to sonication.

To identify the changes occurring in the structure of ultrasonically treated blends, it is also important to analyze the morphological changes taking place with sonication of the blends. It is seen that ultrasonic treatment leads to a higher viscosity matrix (PET). This should enhance the fibrillation of the LCP and improve mechanical properties through the generation of stronger in-situ-reinforced composites. In fact, it is known that matrix polymers having high viscosity typically enhances LCP fibrillation in blends [2, 6, 37, 38]. The effect of ultrasonic treatment on morphology of blends will be discussed in the next section.

Table 1 shows the effect of ultrasonic treatment on the average values of the toughness, impact strength, ultimate strength, Young's modulus and elongation at break of LCP, along with error at 95% confidence intervals. Improvements in mechanical properties were recorded particularly after ultrasonic treatment at an amplitude of 7.5 μm. An average tensile strength of 273 MPa was achieved for LCP treated at an amplitude of 7.5 μm signifying an improvement over the tensile strength of 244 MPa for as-received sample, and 262 MPa for sample extruded without ultrasonic treatment. The higher tensile strength reported above for as-received sample in comparison with the value provided by manufacturer [24] is due to the increased relative thickness of the highly oriented skin region in injection molded mini

tensile bars of the present study in comparison with the standard tensile bars of LCP of previous studies [39, 40]. Average recorded impact strength of pure LCP was 346 kJ/m^2 after ultrasonic treatment at an amplitude of 7.5 μm in contrast to the impact strengths of 244 kJ/m^{2}and 261 kJ/m^2 for the as-received and untreated samples, respectively. Although experimental error should not be disregarded, improvements in the tensile and impact properties of LCP were recorded especially with ultrasonic treatment at an amplitude of 7.5 μm. It should be noted that in studies related to prolong annealing on LCP, other researchers identified solid state polymerization and removal of critical flaws in crystal structure as the causes of increased tenacity of LCP fibers [2, 3, 41-44]. As opposed to heat treatment, the improvements observed in the present study could possibly be due to ultrasonically induced homopolymerization reactions in LCP. It occurs in the melt state at very short residence times, as was observed in the ultrasonic treatment of other polymers [18]. Although dynamic rheological studies did not indicate changes in the dynamic properties of LCP (Figs. 4 and 5), this does not preclude that ultrasonic treatment does not cause rearrangements in molecular structure of LCP through chain scission and recombination reactions. The occurrence of such reactions was observed in PET of the present study and in other polymers [16-19, 22].

Morphology

Injection moldings of LCPs are strongly anisotropic and exhibit skin-core morphology [45]. In general, the skin thickness covers a substantial fraction of the injection molded mini tensile bars [39, 40]. Similar to LCP, SEM micrographs of PET/LCP moldings also revealed skin-core morphology. In these moldings, the core region contained spherical LCP droplets and the skin region of substantial thickness shows highly elongated LCP fibrils of various diameters.

The main factors affecting blend morphology are composition, viscosities of the blend components and the interfacial adhesion between them. It is governed by Taylor's droplet deformation criterion [46]. Although this criterion was derived for small deformation of Newtonian fluids containing low

concentration of droplets, it can be used to estimate the onset of deformation of LCP droplets into fibrils [47].

To express the extent of deformation, the following quantities are defined [46, 47]:

$$p = \frac{\eta_d}{\eta_m} \qquad D = \frac{L - B}{L + B} \qquad Ca = \frac{\eta_m a \dot{\gamma}}{\sigma} \tag{1}$$

where p is the viscosity ratio, η_d and η_m are the steady state viscosity of dispersed and matrix phase, respectively; D is the extent of deformation, L is the length and B the width of the dispersed droplet; Ca is the capillary number defined by the ratio of viscous and interfacial stresses. The capillary number is expressed in terms of an initial droplet radius, a, interfacial tension, σ, and shear rate, $\dot{\gamma}$, with the interfacial stress given by σ/a.

Taylor showed that at very low capillary numbers where the interfacial stress effect dominates, the deformation D can be expressed as follows [46, 47]:

$$D = Ca \frac{19p + 16}{16p + 16} \tag{2}$$

Accordingly, Eq. 2 can be used to calculate droplet deformation in cases of low shear stress occurring in the region close to the centerline in injection molding. In this region, the core morphology is determined by capillary number which is related to interfacial tension between the LCP and PET phases. Therefore, it is expected that in compatibilized blends a greater deformation of the dispersed phase would occur. On the other hand, when Ca=1 and the viscosity ratio p is very large, Taylor expressed deformation as [46]:

$$D = \frac{5}{4p} \tag{3}$$

While the final fibril diameter cannot be predicted because of the constraint of small deformations for which the criteria was derived, it is clear that the droplet deformation is enhanced when the size of

droplets and the viscosity ratio of the matrix to the dispersed phase are large. It should be noted that the viscosity ratio in the fibrillation criteria presented above is based on steady state viscosities of dispersed and matrix phases. Also, Cox-Merz rule is not applicable to LCP and PET/LCP blends, but it is applicable for PET phase. The complex viscosity of LCP is typically higher than its steady state viscosity. Therefore, the value of viscosity ratio p is expected to be lower thus creating more favorable conditions for LCP fibrillation in blends. In addition, since viscosity of PET is shown to increase with ultrasonic treatment at an amplitude of 7.5 μm, the value of p would further decrease, leading to enhancement of LCP fibrillation. Although, strictly speaking, one cannot make quantitative calculations of the aspect ratio of fibrils using the complex viscosity data, qualitative discussions based on Taylor's criterion are still valid and support the morphological observations.

In addition to Taylor's deformation criterion, the energy-based LCP fibrillation criterion [6] can also be used to understand the deformation taking place in LCP/thermoplastic blends. According to this criterion, fibrillation occurs when the energy utilization per unit volume of the thermoplastic component is less than that of the LCP component in the blend:

$$\frac{\dot{E}_m}{\dot{E}_d} = \frac{\dot{\gamma}_m \phi_m}{\dot{\gamma}_d \phi_d} = \frac{\eta_d \phi_m}{\eta_m \phi_d} < 1 \qquad (4)$$

where $\dot{E}_i$ is the rate of energy utilization, $\dot{\gamma}_i$ the shear rate, ϕ_i the volume fraction, and η_i the viscosity of the two phases.

Summarizing the above discussion of LCP fibrillation criteria, it is expected that greater deformation of LCP droplets should occur in blends having a) high LCP content, b) high viscosity ratio of the matrix to the LCP, c) high interfacial adhesion between the matrix and LCP. Therefore, in LCP/thermoplastic blends, fine fibrillar morphology may be obtained when the viscosity of the thermoplastic matrix is higher than that of the LCP. For PET/LCP blends, the viscosity of PET is lower than that of the LCP for the range of ω = 0.1-100 s^{-1} (see Fig. 4). Since LCP is highly shear thinning and PET exhibits

Newtonian behavior, it is expected that at high shear rates encountered during injection molding the viscosities of the two components could be closer with LCP viscosity still being higher than that of PET. The viscosity of PET was shown to increase with ultrasonic treatment at an amplitude of 7.5 μm. Therefore, the deformation of LCP phase by PET is expected to be greater in ultrasonically treated blends. Moreover, due to compatibilization effect by possible copolymer formation during ultrasonic treatment, deformation of the LCP phase in ultrasonically treated blends is expected to be greater.

The following observations of blend morphology provide some experimental evidences of the occurrence of the above discussed effects. In particular, Fig. 8 shows the SEM micrographs of the skin and core regions of 90/10 PET/LCP blends without and with ultrasonic treatment at an amplitude of 7.5 μm. In core and skin regions, LCP droplets and fibrils were observed, respectively. In the absence of ultrasonic treatment, the surface of LCP droplets in the core region is smooth, indicating little interaction with PET. On the other hand, the blend treated at an amplitude of 7.5 μm showed hairy structures on the surface of LCP droplets in the core region, indicating improved adhesion between the PET and LCP phases.

Fig. 9 shows SEM micrographs of the core regions of 80/20 and 70/30 PET/LCP blends without and with ultrasonic treatment at an amplitude of 7.5 μm. The average droplet size of LCP in the core of injection moldings is seen to decrease with increasing LCP concentration in the blends. This is consistent with the droplet deformation criterion of Eq. 4. Moreover, the surface of LCP droplets in the core of blends containing 20 and 30% LCP exhibits hairy structures without and with ultrasonic treatment. However, the size of LCP droplets in the core was lower in blends ultrasonically treated at an amplitude of 7.5 μm, in contrast to those without treatment. Smaller LCP droplets in the core of ultrasonically treated blends (Figs. 9b and 9d), and the presence of hairy structures in ultrasonically treated blend containing 10% LCP (Fig. 8a) affirm that deformation of the LCP phase and its compatibility with PET matrix are improved with ultrasonic treatment.

Fig. 10 shows SEM micrographs of core and skin regions of 90/10 (a, c) and 80/20 PET/LCP (b, d) blends processed at a flow rate of 1 kg/hr and treated at an ultrasonic amplitude of 10 μm. Hairy structures on the surface of LCP droplets were observed in the core (Figs. 10a and 10b). The latter indicates improved interfacial adhesion between PET and LCP. Also, almost no fibrils were seen in the skin region of both blends (Figs. 10c and 10d). Instead small LCP droplets were observed in both skin and core regions. In 90/10 PET/LCP blend, LCP droplets in skin and core regions were smaller than those in 80/20 blend. Evidently, these small LCP droplets in the skin were created by break up of LCP fibrils. However, the stresses generated by ultrasonically treated PET matrix of reduced viscosity at an amplitude of 10 μm were unable to effectively deform these small LCP droplets into fibrils.

SEM micrographs of Fig. 11 provide a comparison of the morphology of 80/20 PET/LCP blends ultrasonically treated at an amplitude of 7.5 μm and flow rates of 1 kg/hr (a, c) and 0.5 kg/hr (b, d). It should be noted that the injection molding conditions dictating final blend morphology were the same in both cases. At a flow rate of 0.5 kg/hr, dispersion in the blend is expected to be poorer than that at a flow rate of 1 kg/hr. Furthermore, the extent of homo and copolymerization reactions induced by ultrasound is expected to be greater at the longer mean residence time of 14 s at a flow rate of 0.5 kg/hr in contrast to 7 s at a flow rate of 1 kg/hr. Comparing Fig. 11a and 11b, it is seen that LCP droplet sizes in the core are larger indicating poor LCP droplet deformation at a flow rate of 0.5 kg/hr corresponding to a mean residence time of 14 s. This is due to the fact that the viscosity of PET at high amplitude and long residence time is significantly reduced due to PET degradation. At the same time, copolymerization may take place at this processing condition leading to improved interfacial adhesion causing hairy structures on LCP droplet surfaces, as indicated in Fig. 11b. Micrographs of the skin regions reveal that the numerous LCP fibrils seen at a mean residence time of 7 s (Fig. 11c) are replaced by fewer fibrils and large undeformed LCP droplets at a residence time of 14 s (Fig. 11d). Clearly, the extent of deformation and number of LCP fibrils in the skin region of moldings are lower for the blend obtained at the longer

residence time in ultrasonic treatment zone. These results indicate that while ultrasonic treatment can improve the interfacial adhesion of PET/LCP blends through in situ compatibilization, its effect on the viscosity of the matrix determines the extent of LCP phase deformation.

Conclusions

PET/LCP blends become stronger, stiffer and more brittle with the addition of LCP. The blends exhibited greater shear thinning behavior with increased LCP content. The viscosity of 90/10 PET/LCP blends was below those of its components indicating that LCP acted as a processing aid. After ultrasonic treatment at an amplitude of 7.5 μm, PET and PET/LCP blends showed an increased viscosity and changes in storage vs. loss modulus behavior. This increased viscosity is an indication of the occurrence of homopolymerization of PET and copolymerization of blends at a short residence times of ultrasonic treatment.

Mechanical properties of LCP increased with ultrasonic treatment at an amplitude of 7.5 μm, indicating possible structural changes in LCP during this treatment. However, rheological measurements were unable to detect these changes. The ultimate strength, Young's modulus, toughness and impact strength of 80/20 PET/LCP blend treated at an amplitude of 7.5 μm and the toughness of 90/10 PET/LCP blend treated at an amplitude of 10 μm were improved due to improved LCP fibrillation and interfacial adhesion with ultrasonic treatment at a residence time of 7 s, as indicated by morphological studies.

In 90/10 PET/LCP blends, the presence of hairy structures on the surface of LCP droplets, indicating interfacial adhesion, were observed with ultrasonic treatment at amplitudes of 7.5 and 10 μm, but not without treatment. Without ultrasonic treatment, sizes of the LCP droplets and fibrils, respectively, in the core and skin regions of molding were reduced with increasing LCP content in the blends. Hairy structure on the surface of LCP droplets in moldings of untreated and treated 80/20 and 70/30 PET/LCP blends were also observed. Such structures were more pronounced in 80/20 blends treated at an

ultrasonic amplitude of 7.5 μm and a mean residence time of 14 s. In this blend, large size hairy droplets and reduced fibrillation of LCP were observed.

The change in PET to LCP viscosity ratio and the compatibilization of PET/LCP blends through ultrasonically induced homopolymerization, copolymerization and degradation reactions determined the morphology and mechanical properties. The amplitude and duration of ultrasonic treatment are decisive factors in the improvement of mechanical properties of these blends. The single step ultrasonic extrusion process for polymer blending was shown to improve interfacial adhesion and fibrillation behavior of PET/LCP blends in the melt state at short residence times. Further refinement of processing conditions could allow one to achieve greater enhancements in the performance of LCP, and its blends with PET.

References

1. Akhtar, S.; Isayev, A. I., "Self-reinforced composites of two thermotropic liquid-crystalline polymers," *Poly. Eng. Sci.*, **33,** 32 (1993).
2. Isayev, A. I. in "*Liquid Crystalline Polymer Systems Technological Advances*," Isayev, A. I.; Kyu, T.; Cheng, S. Z. D. Eds., ACS Symp. Ser. 632, Washington D.C., pp. 1-20 (1996).
3. Calundann, G. W.; Jaffe, M., "Anisotropic polymers, their synthesis and properties," *Proc. R. A. Welch Conf. Chem. Res., Houston, TX*, **45,** 246 (1982).
4. Donald, A.; Windle, A.; Hanna, S., "*Liquid Crystalline Polymers,"* Cambridge: Cambridge University Press, 2005.
5. Qin, Y.; He, J., "Segmented liquid crystalline copolymers and blending with engineering plastics," *Polymer J.,* **26,** 1309 (1994).
6. Joshi, S. C.; Lam, Y. C.; Yue, C. Y.; Tam, K. C.; Li, L.; Hu, X., "Energy-based predictive criterion for LCP fibrillation in LCP/thermoplastic polymer blends under shear," *J. of Applied Polym. Sci.,* **90,** 3314 (2003).
7. Radmard, B.; Dadmun, M. D., "Effect of transesterification on the morphology and mechanical properties of a blend containing a liquid crystalline polymer," *J. Appl. Polym. Sci.*, **80,** 2583 (2001).
8. Pedretti, U.; Roggero A; La Mantia; F. P.; Magagnini, P. L., "Semiflexible liquid crystalline copolyesters and their blends with commercial thermoplastics," *SPE Antec Technical Papers*, 1706 (1993).
9. Wu, C.; Han, C. D.; Suzuki, Y.; Mizuno, M., "Transesterification and Mechanical Properties of Blends of a Model Thermotropic Polyester and Polycarbonate," *Macromolecules*, **39,** 3865 (2006).
10. Heino, M. T.; Seppälä, J. V., ""The effect of mixing time and catalyst addition on the compatibility of PET/LCP blends," *Acta Polytech. Scand., Chem. Technol. Ser. 214*, Helsinki, pp.

1-25 (1993).

11. Chin, H. C.; Chiou, K. C.; Chang, F. C., "Reactive compatibilization of the poly(ethylene terephthalate)/liquid crystalline polymer blends by solid epoxy resin as a coupling agent," *Journal of Appl. Polymer Sci.,* **60,** 2503 (1996).
12. Kobayashi, T.; Sato, M.; Takeno, N.; Mukaida, K. I., "Compatibilizing effect of a thermotropic liquid-crystalline compatibilizer on liquid-crystalline polycarbonate/poly(p-phenylene oxide) blends," *Macromol. Chem. Phys.,* **195,** 2771 (1994).
13. Schleeh, T.; Salamon, L.; Hinrichsen, G.; Kossmehl, G., "Blends of alkyloxy-substituted liquid-crystalline aromatic polyesters and copolyesters with poly(ethylene terephthalate)," *Makromol. Chem.,* **194,** 2771 (1993).
14. Kwon, S. K.; Chung, I. J., "Molecular structure effect of thermotropic liquid crystalline polymers on interfacial adhesion with polycarbonate," *Polym. Compos.,* **16**, 297 (1995).
15. Chen, Sr.; P., Sullivan, V.; Dolce, T.; Jaffe, M., "Compatible LCP blends with direct esterification," *US5,182,334* (1991).
16. Isayev, A. I..; Hong, C. K.; Kim, K. J., "Continuous mixing and compounding of polymer/filler and polymer/polymer mixtures with the aid of ultrasound," *Rubber Chem. Technol.*, **76,** 923-947 (2003).
17. Lin, H.; Isayev, A. I., "Ultrasonic treatment of polypropylene, polyamide 6, and their blends," *J. Appl. Polym. Sci.*, **102,** 2643 (2006).
18. Isayev, A. I., "Chapter 15: Rubber recycling," in *Rubber Technologist's Handbook,* Eds. White, J. R.; De, S. K., UK: RAPRA Technology Ltd., pp. 511-547 (2001).
19. Isayev, A. I.; Hong, C. K., "Ultrasound assisted continuous process for making polymer blends and copolymers," *U.S. Pat. 6,528,554* (2003).
20. Margulis, M. A., translated by Leib, G., *"Sonochemistry and Caviation,"* Amsterdam: Gordon and

Breach Science Publishers SA (1995).

21. Price, G. J. in *"New methods of polymer synthesis, Vol. 2,"* Ebdon, J. R.; Eastmond, G. C. Eds., London: Chapman & Hall, pp. 117-160 (1995).
22. Isayev, A. I.; Hong, C. K., "Novel ultrasonic process for in situ copolymer formation and compatibilization of immiscible polymers," *Polym. Eng. Sci.,* **43,** 91-101 (2003).
23. Kyotani, M.; Kaito, A.; Nakayama, K., "Mechanical and structural properties of extruded strands of blends containing a liquid-crystalline polyester with poly(ethylene terephthalate)," *Polymer,* **33,** 4756-62 (1992).
24. *Vectra A950 – Datasheet*, Ticona (2007).
25. Wissbrun, K. F.; Kiss, G.; Cogswell, F. N., "Flow behavior of a thermotropic liquid crystal aromatic copolyester," *Chem. Eng. Comm.,* **53,** 149-173 (1987).
26. Wissbrun, K. F., "Rheology of rod-like polymers in the liquid crystalline state," *J. Rheol.,* **25,** 619-662 (1981).
27. Giles, D. W.; Denn, M. M., "The effect of suppression of offgassing on the rheometry of thermotropic liquid crystalline polymers," *J. Rheol.,* **38,** 617-637 (1994).
28. Cogswell, F. N., Wissbrun, K. F. in *"Rheology and Processing of Liquid Crystal Polymers,"* Acierno, D., Collyer, A. A. eds., 86-134, New York: Chapman & Hall (1996).
29. Gotsis, A. D.; Baird, D. G., "Rheological properties of copolyester liquid crystalline melts. II. Comparison of capillary and rotary rheometer results," *J. Rheol.*, **29,** 539 (1985).
30. Kim, W. N.; Denn, M. M., "Properties of blends of a thermotropic liquid crystalline polymer with a flexible polymer (Vectra/PET)," *J. Rheol.*, **36,** 1477 (1992).
31. Cogswell, F. N.; Griffin, B. P.; Rose, J. B., "Compositions of melt-processable polymers having improved processibility, and method of processing," *Eur. Pat. 0030417* (1981).
32. Cole, K. S.; Cole, R. H., "Dispersion and absorption in dielectrics. I. Alternating-current

characteristics," *J. Chem. Phys.,* **9,** 341-51 (1941).

33. Masuda, T.; Ohta, Y.; Onogi, S., "Rheological properties of anionic polystyrenes. III. Characterization and rheological properties of four-branch polystyrenes," *Macromolecules,* **4,** 763-768 (1971).

34. Harrell, E. R.; Nakajima, B. F. "Modified Cole-Cole plot based on viscoelastic properties for characterizing molecular architecture of elastomers." *J. Appl. Polym. Sci.,* **29,** 995-1010 (1984).

35. Han, C. D.; Yang, H. H., "Rheological behavior of blends of poly(methyl methacrylate) (PMMA) and poly(acrylonitrile-stat-styrene)-graft-polybutadiene (ABS)," *J. Appl. Polym. Sci.,* **33,** 1221-1229 (1987).

36. Han, C. D.; Yang, H. H., "Rheological behavior of compatible polymer blends. I. Blends of poly(styrene-co-acrylonitrile) and poly(ϵ-caprolactone)," *J. Appl. Polym. Sci.,* **33,** 1199-1220, (1987).

37. Lin, Q.; Jho, J.; Yee, A. F., "Effect of drawing on structure and properties of a liquid-crystalline polymer and polycarbonate in-situ composite," *Polymer Eng. and Sci.,* **33,** 789-798 (1993).

38. Joslin, S.; Jackson, W.; Farris, R., "A novel TLCP blended with PET and PC matrices," *J. Appl. Polym. Sci.,* **54,** 289-302 (1994).

39. Ophir, Z.; Ide, Y., "Injection molding of thermotropic liquid crystal polymers," *Polym. Eng. Sci.*, **23,** 792 (1983).

40. Thapar H., and Bevis, M., "Processing, property and morphology of an injection molded liquid crystal thermoplastic polymer," *Plast. Rubber Compos. Process. Appl.,* **12,** 39-52 (1989).

41. Yoon, H. N., "Strength of fibers from wholly aromatic polyesters," *Colloid. Polym. Sci.*, **268,** 230 (1990).

42. Yoon, H. N.; Charbonneau, L. F.; Calundann G. W., "Synthesis, processing and properties of thermotropic liquid-crystal polymers," *Adv. Mater.,* **4,** 206-214 (1992).

43. Jaffe, M., "Applications of liquid crystal polymers," *J. Stat Phys.,* **62,** 985 (1991).

44. Sarlin, J.; Törmälä, P., "Isothermal heat treatment of a thermotropic LCP fiber," *J. Polym. Sci., Part B: Polym. Phys.,* **29,** 395 (1991).

45. Sawyer, L.C. and Jaffe M., 1986, "The structure of thermotropic polyesters," *J. Mater. Sci.,* **21,** 1897-1913 (1986).

46. Taylor, G. I., "The Formation of Emulsions in Definable Fields of Flow," *Proc. Roy. Soc.*, A 146, 501 (1934).

47. C. H. Song and A. I. Isayev, "LCP Droplet Deformation in Fiber Spinning Self-Reinforced Composites", *Polymer*, 42, 2611-2619, 2001.

Table 1: Average mechanical properties of untreated and ultrasonically treated LCP with the error indicating 95% confidence intervals.

LCP	virgin	0 μm	5 μm	7.5 μm	10 μm
Ultimate strength (MPa)	244±7	262±7	251±8	273±16	262±6
Modulus (GPa)	8.9±0.3	9.4±1.1	9.1±0.4	10.0±0.5	10.8±0.8
Toughness (MPa)	60±7	58±7	60±7	70±6	53±5
Ultimate strain (%)	37±3	35±3	36±2	37±2	31±2
Impact strength (kJ/m^2)	244±13	261±47	283±82	346±86	292±59

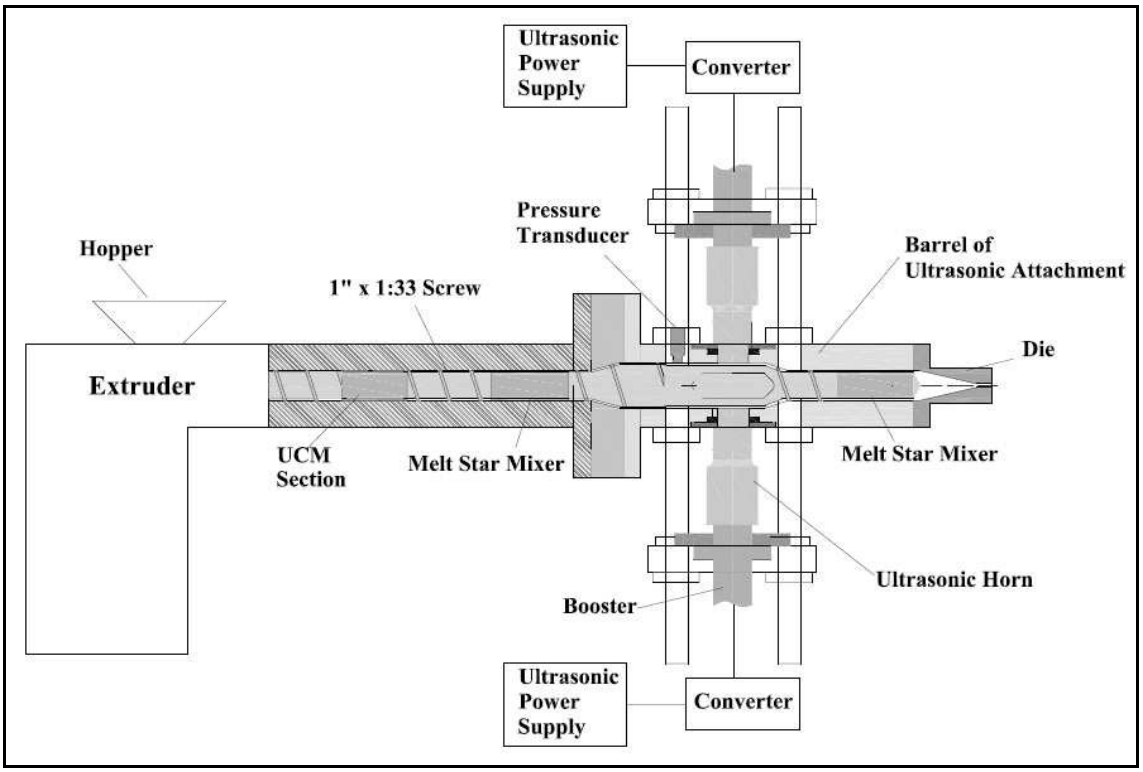

Figure 1. The ultrasonic extruder.

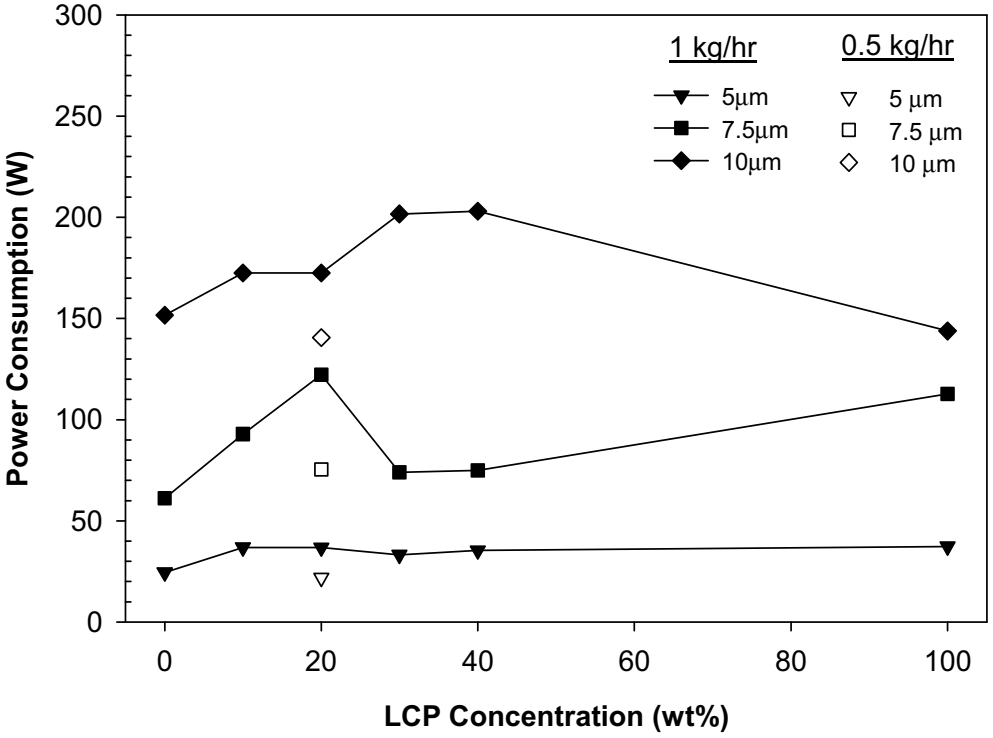

Figure 2. Ultrasonic power consumption at different ultrasonic amplitudes versus LCP concentration at a flow rate of 1 kg/hr. Open symbols are for 80/20 PET/LCP blend at a flow rate of 0.5 kg/hr.

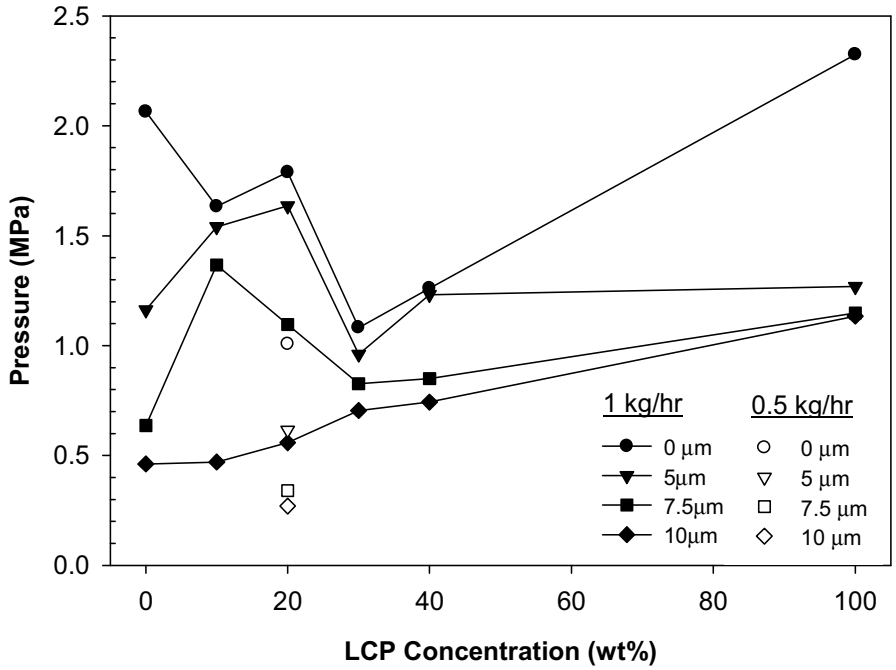

Figure 3. Pressure before ultrasonic treatment zone at different ultrasonic amplitudes versus LCP concentration at a flow rate of 1 kg/hr. Open symbols are for 80/20 PET/LCP blend at a flow rate of 0.5 kg/hr.

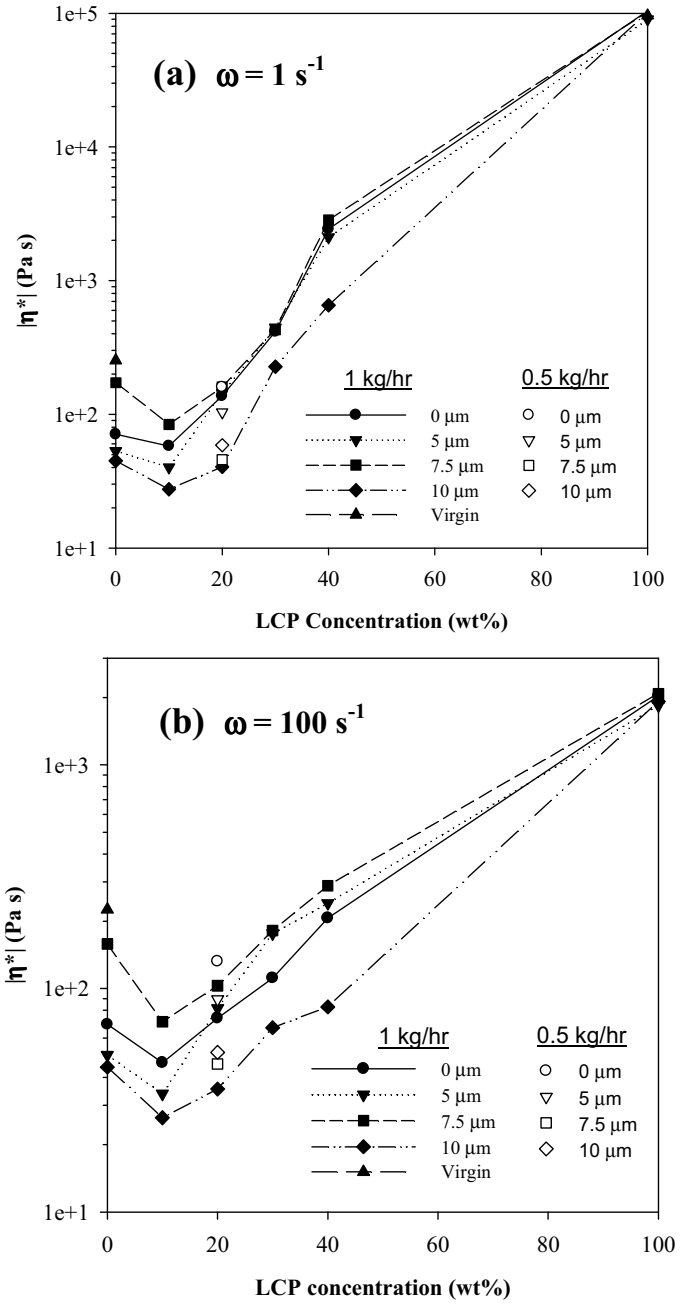

Figure 4. Complex viscosity at different ultrasonic amplitudes versus LCP concentration at frequencies of 1 s^{-1} (a) and 100 s^{-1} (b) at a flow rate of 1 kg/hr. Open symbols are for 80/20 PET/LCP blend at a flow rate of 0.5 kg/hr.

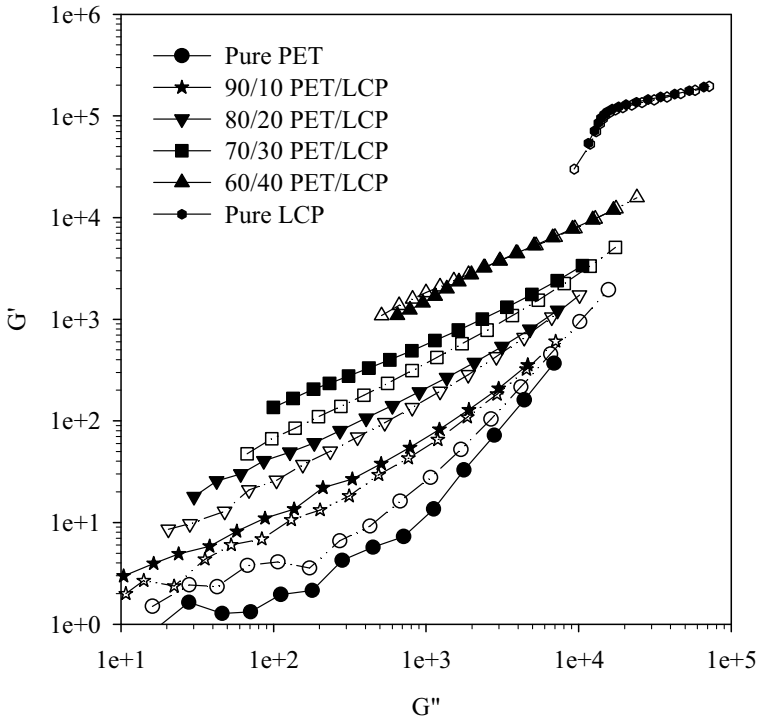

Figure 5. G' versus G" for PET/LCP blends without (filled symbols) and with (open symbols) ultrasonic treatment at an amplitude of 7.5 μm at a flow rate of 1kg/hr.

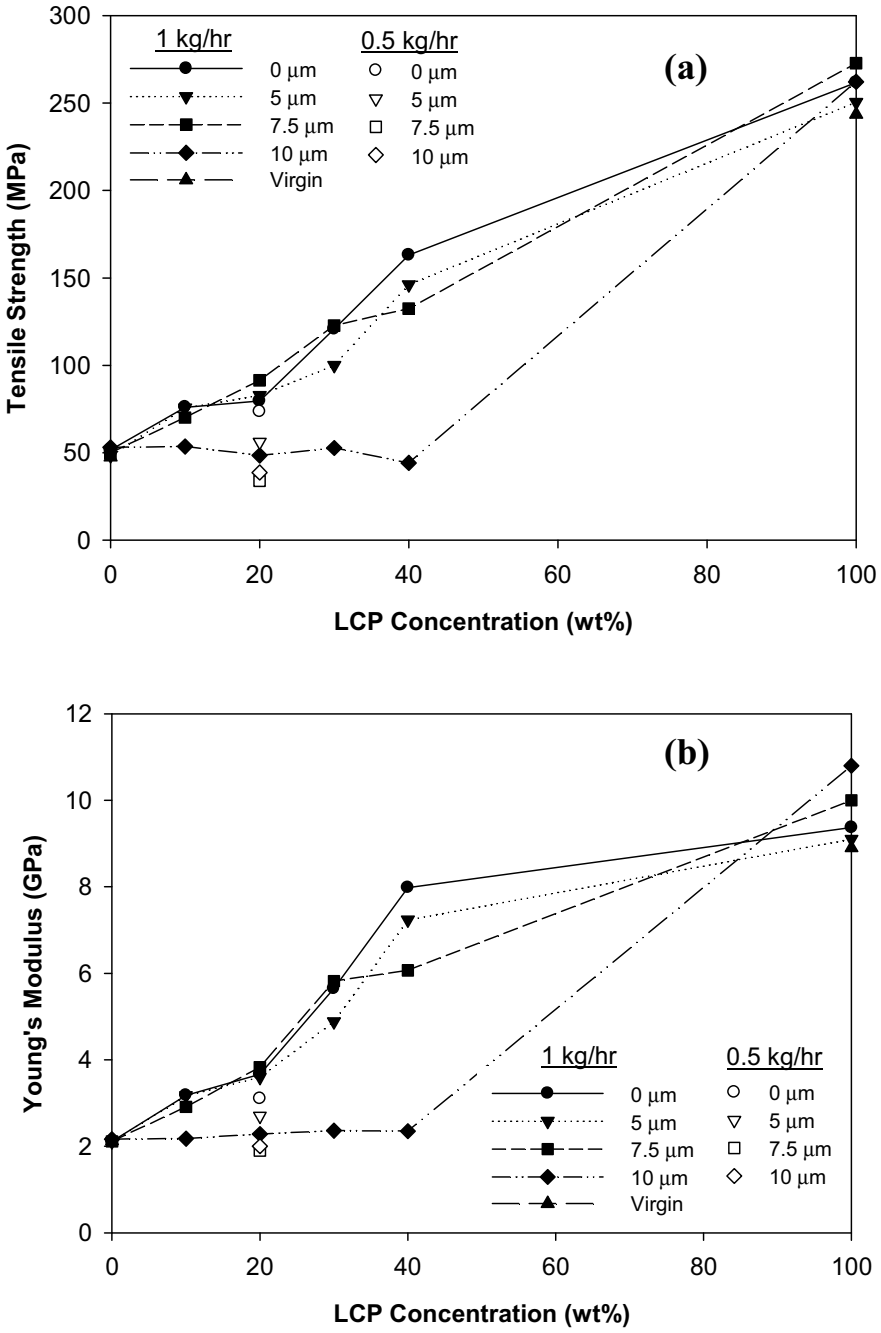

Figure 6. Tensile strength (a) and Young's modulus (b) at different ultrasonic amplitudes versus LCP concentration at a flow rate of 1 kg/hr. Open symbols are for 80/20 PET/LCP blend at a flow rate of 0.5 kg/hr.

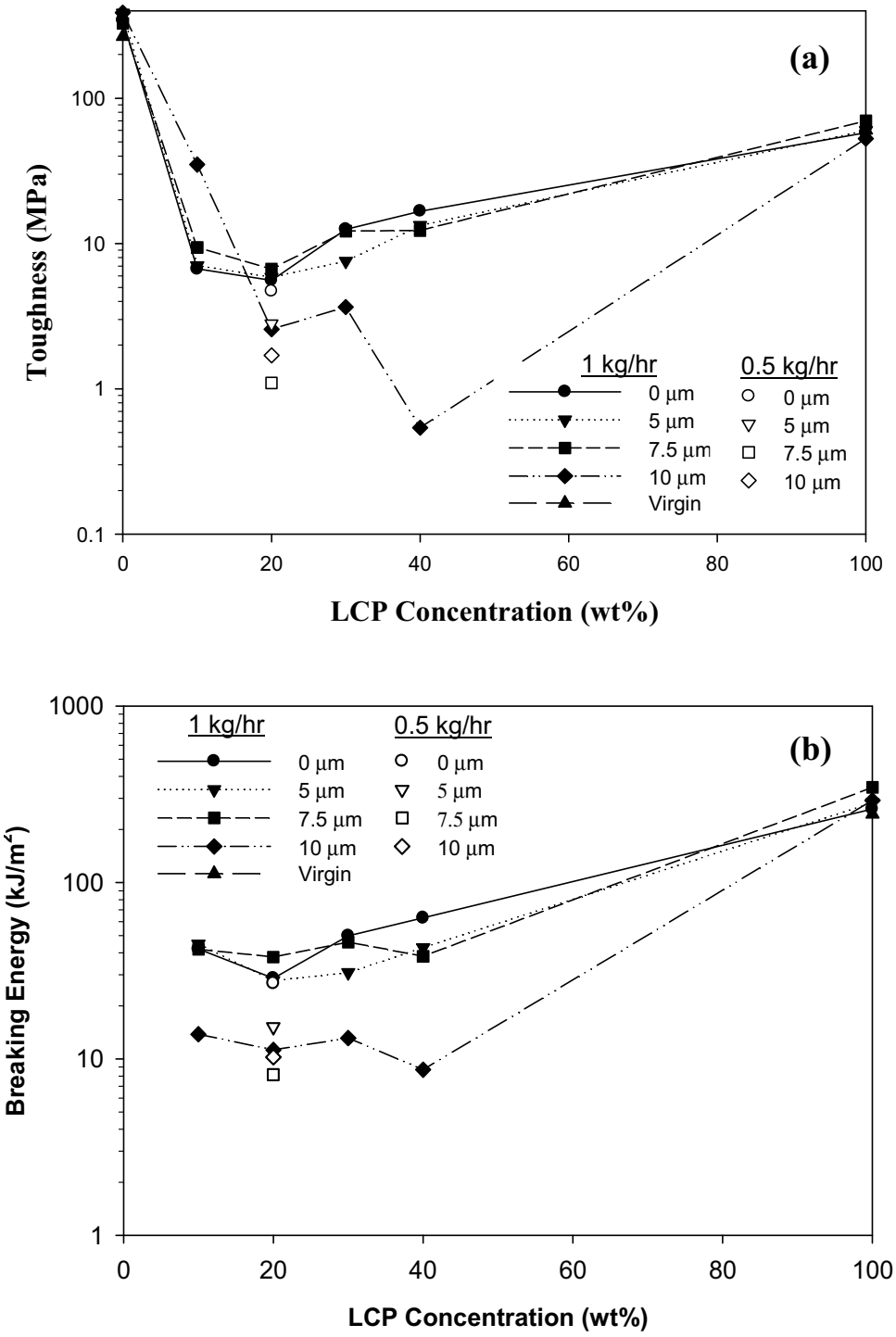

Figure 7. Toughness (a) and impact strength (b) at different ultrasonic amplitudes versus LCP concentration at a flow rate of 1 kg/hr. Open symbols are for 80/20 PET/LCP blend at a flow rate of 0.5 kg/hr.

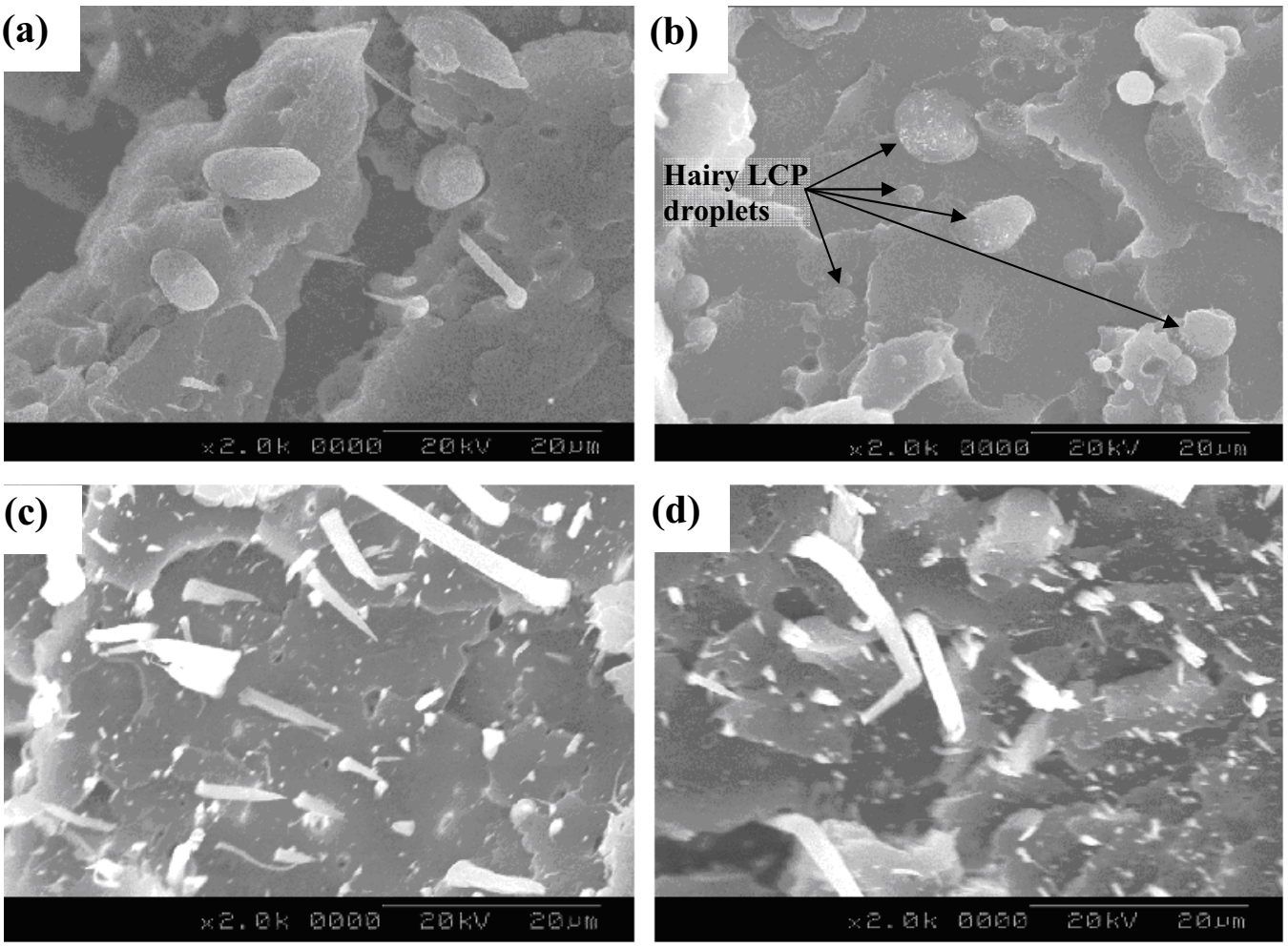

Figure 8. SEM micrographs of 90/10 PET/LCP blends obtained at a flow rate of 1 kg/hr. (a) untreated core region, (b) core region treated at an ultrasonic amplitude of 7.5 μm, (c) untreated skin region, (d) skin region treated at an ultrasonic amplitude of 7.5 μm.

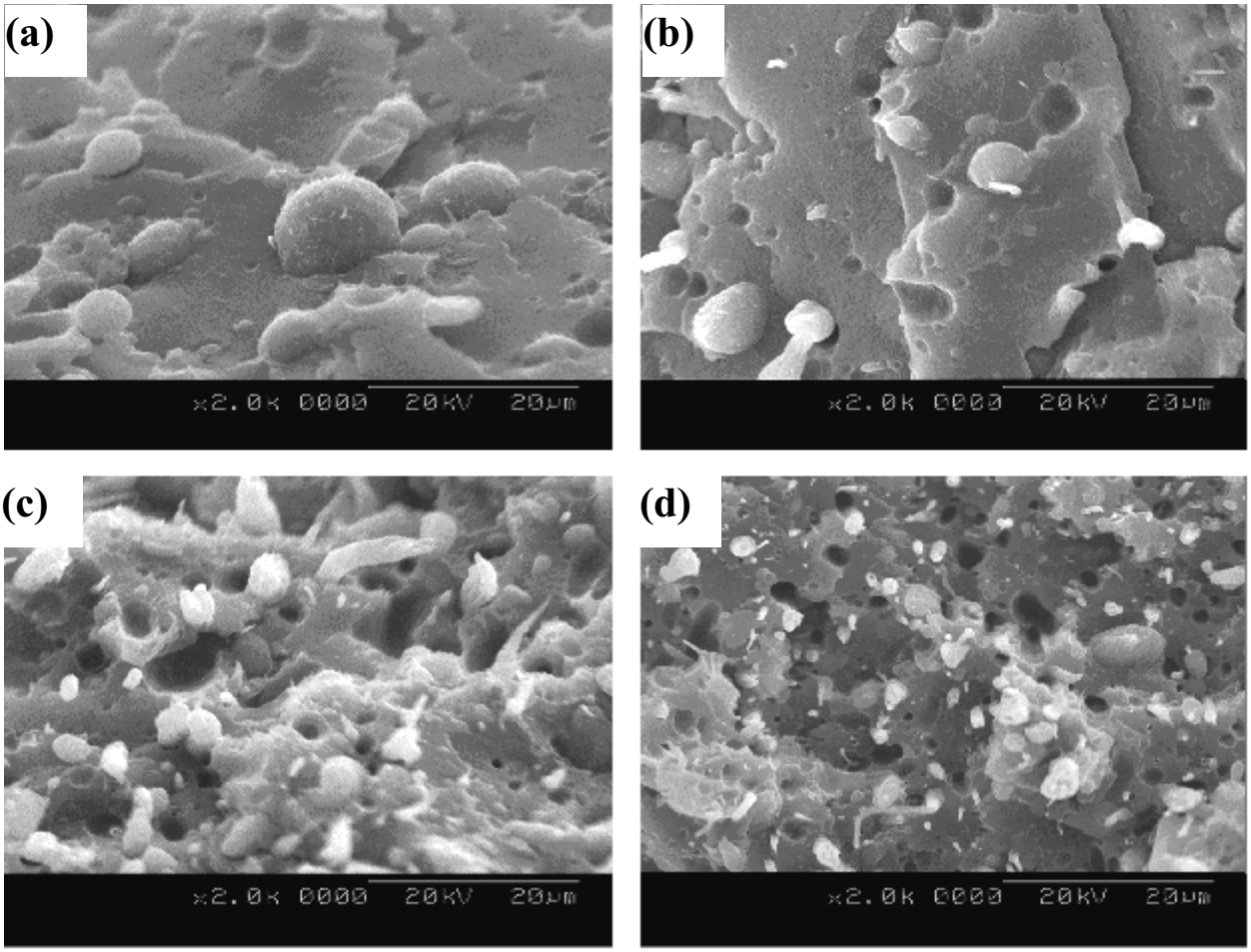

Figure 9. SEM micrographs of core regions obtained at a flow rate of 1 kg/hr. (a) 80/20 untreated, (b) 80/20 treated at an ultrasonic amplitude of 7.5 μm, (c) 70/30 untreated, (d) 70/30 treated at an ultrasonic amplitude of 7.5 μm and.

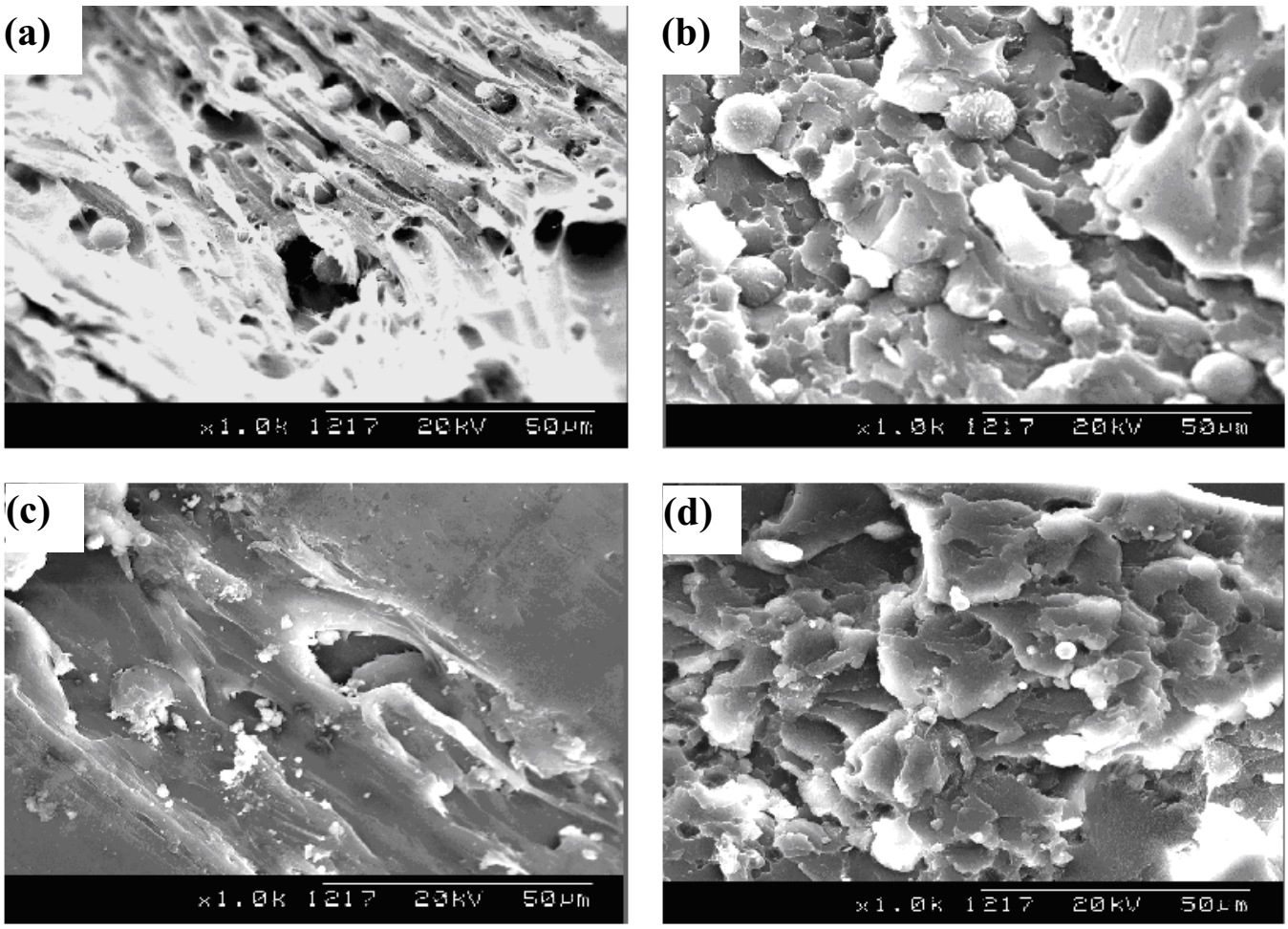

Figure 10. SEM micrographs of PET/LCP obtained at a flow rate of 1 kg/hr and treated at an ultrasonic amplitude of 10 µm. (a) core region of 90/10, (b) core region of 80/20, (c) skin region of 90/10, (d) skin region of 80/20.

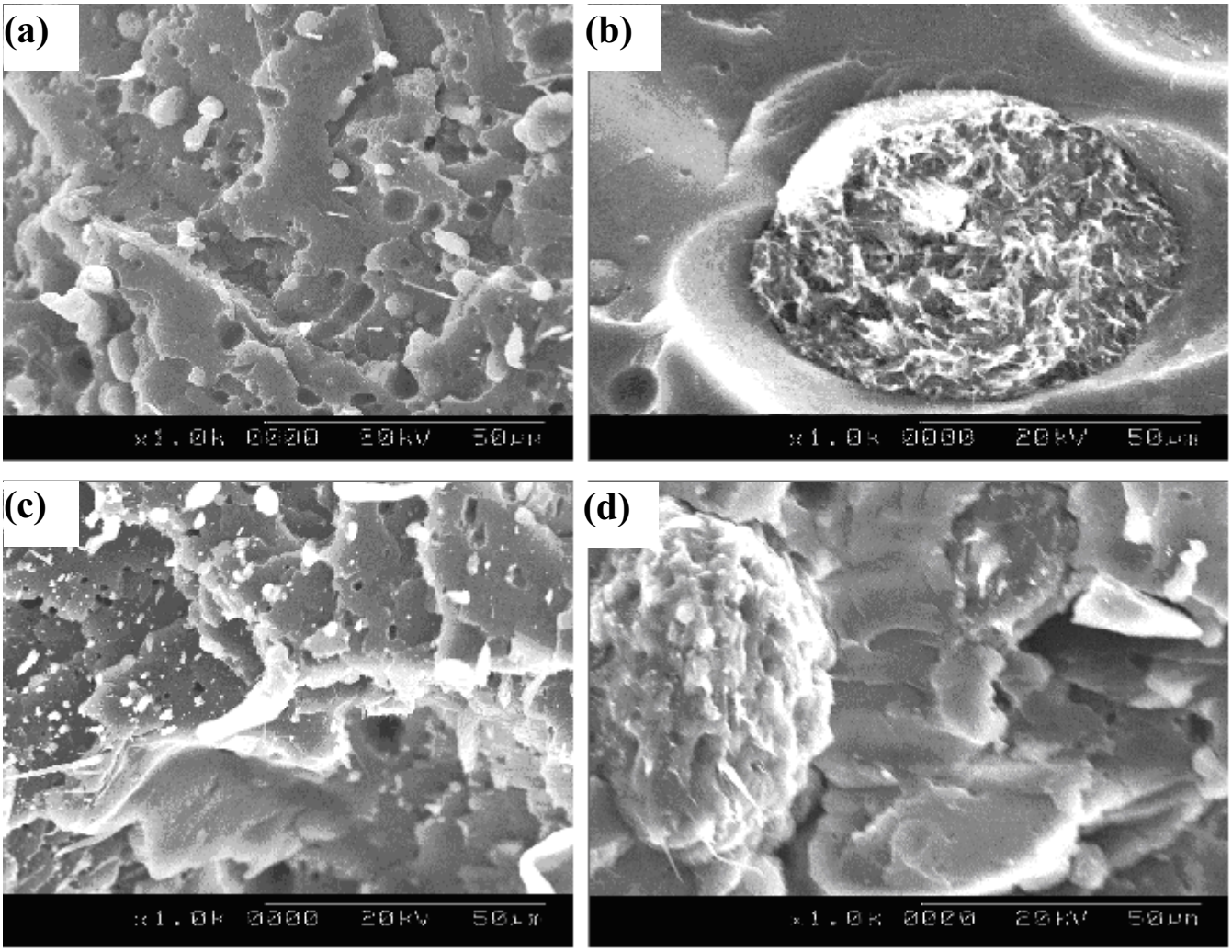

Figure 11. SEM micrographs of 80/20 PET/LCP blends ultrasonically treated at an amplitude of 7.5 μm at different residence times under ultrasonic horns. (a) 7 s (1 kg/hr flow rate), core region. (b) 14 s (0.5 kg/hr flow rate), core region. (c) 7 s (1 kg/hr flow rate), skin region. (d) 14 s (0.5 kg/hr flow rate), skin region.